

# Single-Molecule Kinetics of Interfacial Electron Transfer

H. Peter Lu and X. Sunney Xie\*

Pacific Northwest National Laboratory, Environmental Molecular Sciences Laboratory, P.O. Box 999, Richland, Washington 99352

Received: November 4, 1996; In Final Form: February 5, 1997<sup>⊗</sup>

Measurements of single-molecule chemical reaction kinetics are demonstrated for interfacial electron transfer from excited cresyl violet molecules to the conduction band of indium tin oxide (ITO) or energetically accessible surface electronic states under ambient conditions by using a far-field fluorescence microscope. In this system, each single molecule exhibits a single-exponential electron transfer kinetics. A wide distribution of site-specific electron transfer rates is observed for many single cresyl violet molecules examined. This work reveals that the physical origin of multiexponential kinetics of electron transfer in this system is the inhomogeneity of molecular interactions on the semiconductor surface of ITO. We illustrate that the single-molecule experiments provide detailed information not obtainable from experiments conducted on large ensembles of molecules. Single-molecule kinetics is particularly useful in understanding multiexponential behavior of chemical reactions in heterogeneous systems.

## Introduction

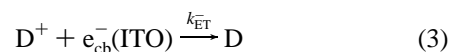
Recent advances in near-field<sup>1–6</sup> and far-field<sup>7–9</sup> fluorescence microscopies have made it possible to image the emission from single molecules with high spatial resolutions and to extend the single-molecule spectroscopy work done at cryogenic temperatures<sup>10</sup> to the room temperature regime.<sup>2–6,8,9</sup> Molecular interactions and chemical dynamics can now be probed in specific local environments. There are two distinctly different time scales on which one can probe single-molecule dynamics. On the millisecond to hundred-second time scale, spectral trajectories<sup>9</sup> and diffusional trajectories<sup>11</sup> of single molecules have been studied. On the picosecond to nanosecond time scale, excited state processes, such as radiative and nonradiative energy transfer processes, have been studied by repetitive excitation with short laser pulses.<sup>4–6,8</sup> In this Letter, we demonstrate an example for measuring chemical kinetics on this fast time scale.

Chemical activity on a single-molecule basis has been a subject of recent studies.<sup>7b,12,13</sup> On a single-molecule basis, all stochastic events of chemical reactions take place on subpicosecond time scales. The rate of chemical reaction can be much slower because of low probabilities for successful crossing of the barrier or transition state. In conventional measurements made on large ensembles of molecules, the rate of chemical reaction is often measured by the rate of concentration change. On a single-molecule basis, the rate of chemical reaction reflects the change of probability rather than concentration. Time-correlated single photon counting experiments on single molecules allow for measurements of the temporal survival probabilities of excited states, which reflect the rates of single-molecule chemical reactions for many photoinduced chemical processes. Such measurements made on a specific local environment can avoid complications associated with site heterogeneity.

Motivated by developments of chemical solar cells and photography, intensive investigations have focused on dye photosensitization on semiconductor surfaces for the last 20 years.<sup>14–22</sup> In a typical dye-photosensitization system, photoexcitation of dye molecules dispersed on the surface of a wide band gap (>2.5 eV) semiconductor<sup>23</sup> results in ejection of

electrons from the dye molecules to the conduction band or energetically accessible surface electronic states of the semiconductor.<sup>24</sup> Multiexponential kinetics of this interfacial electron transfer has been observed by many groups.<sup>25–34</sup> In general, the origin of the multiexponential kinetics is not well understood, and possible mechanisms include dye molecule aggregation and cluster formation,<sup>16,17,28,34</sup> exciton diffusion,<sup>16,17,19,35</sup> and the site heterogeneity of dye molecules and their environments,<sup>16, 17,19,28,29</sup> etc. Identification of the physical nature of multiexponential kinetics is extremely difficult for an ensemble-averaged experiment in these systems.

To demonstrate measurements of single-molecule chemical kinetics and to investigate the physical origins of the multiexponential kinetics in interfacial electron transfer, we examined the system of cresyl violet photosensitization<sup>26,28</sup> on an indium tin oxide (ITO) semiconductor surface.<sup>36</sup>



where the  $e_{cb}^-(ITO)$  represents the electron ejected from the excited cresyl violet molecule ( $D^*$ ) to the conduction band or energetically accessible surface electronic states of ITO. The rate of forward electron transfer,  $k_{ET}$ , can be measured by the fluorescence decay of excited dye molecules.<sup>37</sup> The rate of backward transfer,  $k_{ET}^-$ , is orders of magnitude slower.<sup>14–22,30,31,38</sup> We measured single-molecule interfacial electron transfer rates at specific local environments, providing new insights into the origin of multiexponential behavior.

## Experimental Section

Although a near-field optical microscope (NSOM) is capable of measuring single-molecule electron transfer kinetics free from perturbation of the NSOM tip,<sup>6</sup> fluorescence imaging using a confocal arrangement<sup>7</sup> has superior sensitivity for spectroscopic measurements<sup>8</sup> and is most suitable for studying single-molecule behavior in a dilute sample. The far-field approach, however, sacrifices subdiffraction spatial resolution and the ability to

\* To whom correspondence should be addressed.

⊗ Abstract published in *Advance ACS Abstracts*, March 15, 1997.

correlate spectroscopic information with topographic information, as offered by NSOM. The experiments reported here were performed on very dilute samples using a conventional inverted fluorescence microscope (Nikon, Diaphot 300), similar to that discussed in other recent reports.<sup>8,9</sup>

The output of a mode-locked YAG:Nd laser (Coherent Antares) is frequency doubled to 532 nm (2 W, 80 ps fwhm, 76 MHz) and used to synchronously pump a cavity-dumped dye laser (Coherent 702) operating with Rhodamine 6G lasing at 570 nm. The output of the dye laser (10 ps fwhm pulses train at 8 MHz repetition rate) was passed through a prism to eliminate spontaneous emission and was intensity stabilized by a laser stabilization accessory (Liconix 50SA). A half-wave plate was used to align the linear polarization of the laser light perpendicular to the optic table. The excitation light was attenuated to 0.1–2  $\mu$ W and collimated by an adjustable laser beam collimator (Newport). The beam was sent into the microscope from its back side, reflected up by a dichroic beam splitter (Nikon DM580), and focused by a 60 $\times$  oil immersion objective lens (Nikon, numerical aperture of 1.4) onto the upper sample surface of a microscope cover slip (Fisher Scientific; 0.17 mm thick). The waist of the input excitation beam was adjusted according to the size of the back aperture of the objective lens, ensuring a tight focus spot (diffraction limited,  $\sim$ 340 nm fwhm) at the sample surface. The sample can be raster scanned or moved to a particular position with respect to the laser focus using an  $x$ – $y$  positioning stage.

The fluorescence was collected by the same objective lens through the transmissive sample and was directed to the camera port of the microscope after going through the dichroic beam splitter. The scattered excitation light was cut off by the dichroic beam splitter and two color filters (Schott, RG590, 3 mm thick). The emission was imaged onto a photon-counting avalanche photodiode (EG&G Canada, SPCM-200), the small active area of which (100  $\mu$ m  $\times$  100  $\mu$ m) ensures confocal imaging. Fluorescence lifetime was measured by time-correlated single photon counting with an instrumental response function of 160 ps (fwhm), similar to that previously described.<sup>3c</sup> A spectrograph (Acton 150 with 600 g/mm grating) and a back-illuminated charge coupled device (CCD) camera (Princeton Instruments, LN130) were configured to collect emission spectra with 1 nm resolution. The microscope was in a dark compartment, and the system was on an air-floated optic table. All measurements were conducted under ambient conditions.

ITO films in hundreds of nanometer thicknesses (sheet resistance is ca. 220  $\Omega$ /cm<sup>2</sup>) were sputter coated on microscope cover slips under an Ar atmosphere (CrC-100 Sputtering System, Plasma Sciences Inc.). The ITO target material (99.99% pure) was purchased from Kurt J. Lesker Company. The topographic features of the ITO films were examined by an atomic force microscope (AFM) (Digital Instruments, NanoScope III). The samples were prepared by spin coating (5000 rpm) a dilute cresyl violet methanol solution ( $10^{-9}$  M) onto the ITO films. An air-dried sample was further covered with a 20 nm poly(methyl methacrylate) (PMMA) film (spin coated with dilute PMMA dichloromethane solution;  $10^{-1}$  g/L) in order to prevent fast photobleaching. The cresyl violet was purchased from Exiton. PMMA, methanol, and dichloromethane were analytical reagents from Aldrich.

## Results and Discussion

Figure 1 shows a 5  $\mu$ m  $\times$  5  $\mu$ m fluorescence image of single cresyl violet molecules dispersed on an ITO surface. Each individual feature in Figure 1 is attributed to a single cresyl violet molecule, evidenced by the polarized emission and sudden

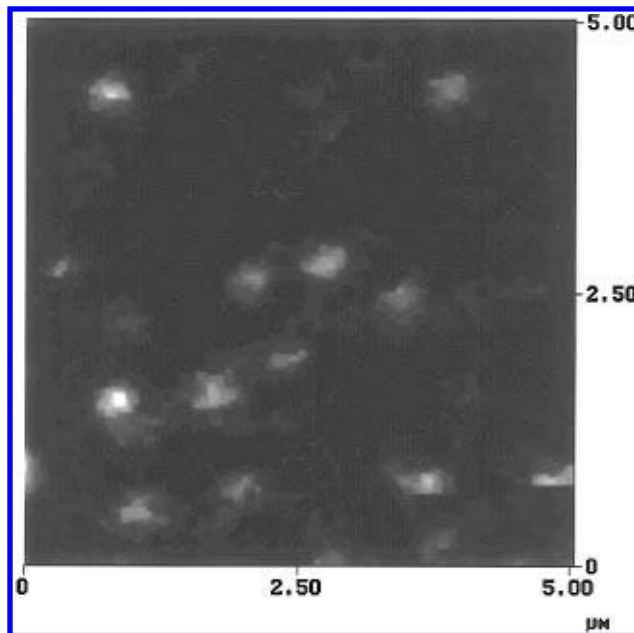


**Figure 1.** Fluorescence image (5  $\mu$ m  $\times$  5  $\mu$ m) of single cresyl violet molecules dispersed on the surface of an indium tin oxide (ITO) film. This image was taken in 4 min with an inverted fluorescence microscope. Each individual feature is attributed to a single cresyl violet molecule. The intensity variation between the molecules is due to different molecular orientations, excitation spectra, and emission quantum yields. The emission spectrum and fluorescence decay of a single molecule are measured after placing the single molecule on the diffraction limited focus spot (340 nm fwhm).

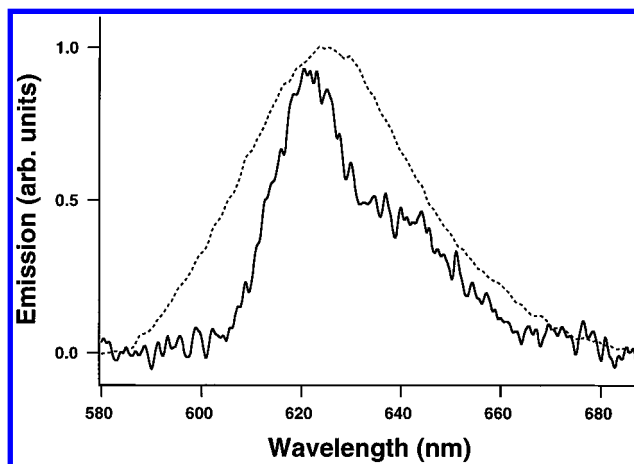


**Figure 2.** Single-molecule emission spectrum (solid line) of a cresyl violet molecule on indium tin oxide (ITO) surface and the ensemble-averaged emission spectrum (dashed line). The single-molecule spectrum was taken with 570-nm excitation in 5 s. The ensemble-averaged spectrum was taken with 550-nm excitation by using a fluorometer (SPEX 1680).

quantized disappearance of the signal as a result of photobleaching. The intensity variation between the molecules results from different molecular orientations, excitation spectra, and emission quantum yields. The intensities of the molecules were about an order of magnitude weaker than the intensities of cresyl violet molecules dispersed on a cover slip without ITO coating under the same experimental conditions. The weaker signal intensities result from the significantly lower emission quantum yield, which will be discussed later in this text.

Figure 2 shows an ensemble-averaged emission spectrum (dashed line) of cresyl violet on ITO surface and a single-molecule emission spectrum (solid line) of a particular cresyl violet molecule. The ensemble-averaged spectrum is not noticeably different from that of cresyl violet on a glass cover slip, indicating a weak vibronic coupling between the cresyl

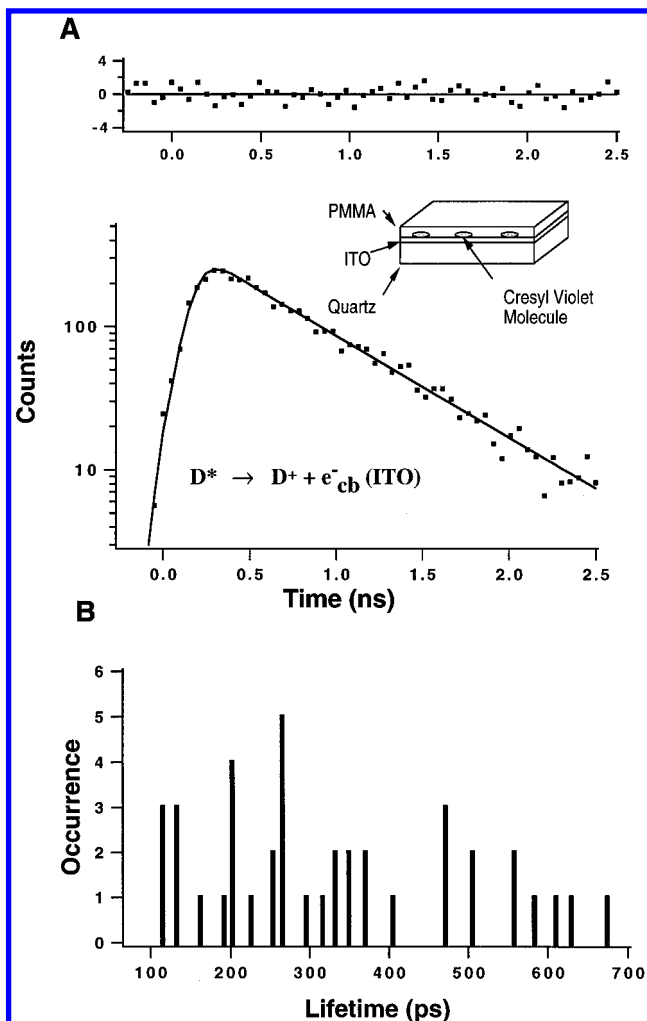


**Figure 3.** (A) Fluorescence decay of a single cresyl violet molecule dispersed on an indium tin oxide (ITO) film, measured by time-correlated photon counting. The solid line is the fitted decay (single exponential of  $480 \pm 5$  ps with  $\chi^2 = 1.14$ ) convoluted with the instrumental response function (fwhm 160 ps). Weighted residuals are shown at the top. The single-exponential decay is due to interfacial electron transfer from the excited molecule ( $D^*$ ) to the conduction band or energetically accessible surface electronic states of ITO. (B) Distribution of single-molecule emission lifetimes for 40 different molecules. A broad distribution of site-specific electron transfer kinetics is observed.

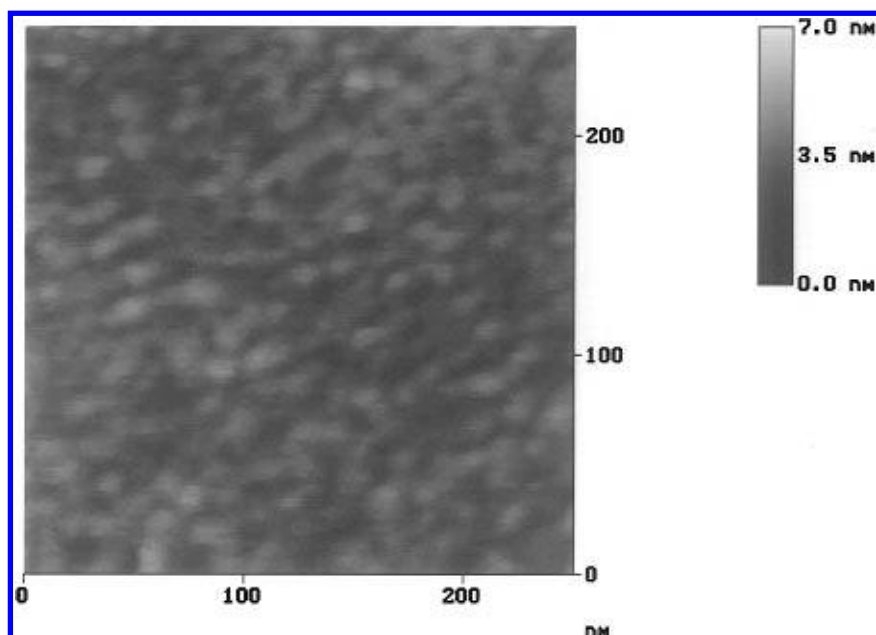
violet and ITO. Due to inhomogeneity of different sites, the single-molecule spectrum is narrower. The vibronic feature, not evident in the ensemble-averaged spectrum, is clearly present in the single-molecule spectrum. Among many single-molecule spectra examined (not shown) there is a broad distribution of peak positions (between 615 and 630 nm).

Figure 3A displays the fluorescence decay of a single cresyl violet molecule on ITO, which is single exponential with a time constant of 480 ps. Measured under the same experimental conditions, the emission lifetimes of single cresyl violet molecules dispersed on a glass cover slip were 2.5–3 ns, which were the radiative lifetimes. Radiative rates of single molecules are known to depend on transition frequency, dipole orientation, and dielectric constant of the substrate.<sup>8,39</sup> Although the higher index refraction of the ITO surface ( $n_{\text{ITO}} = 2.05$ ) than that of glass ( $n_{\text{glass}} = 1.52$ ) should result in a larger radiative rate for a flat ITO surface,<sup>39</sup> it is unlikely that the fast decay in Figure 3A is due to the radiative process. We attribute the decay in Figure 3A to nonradiative processes.

Several possible nonradiative processes were considered: (1) energy transfer from the dye molecules to the semiconductor was precluded in considering that absorption is negligible for ITO in wavelengths longer than 570 nm; (2) dye-to-dye energy transfer (exciton diffusion and annihilation) is not possible at such low coverage (see Figure 1); (3) the charge transfer from dye molecules to PMMA polymer by the charge-transfer-to-solvent mechanism<sup>40</sup> is ruled out because similar lifetimes were also observed on samples not covered with PMMA. Therefore, we attribute the fast decay in Figure 3 to the interfacial electron transfer. Similar interfacial electron transfer rates have been seen on similar systems.<sup>25,27–33</sup>

In this system, electron transfer kinetics is single exponential for all the single molecules examined. There were no noticeable changes of emission lifetimes during the course of measurements. We note that multiexponential kinetics would be possible for single molecules, if, for example, variations of molecular nuclear coordinates occurred during the course of measurements ( $10^{-2}$ – $10^2$  s) through spontaneous or photoinduced mechanisms.<sup>9</sup> However, we did not observe the multiexponential kinetics on single molecules in this system.

Figure 3B shows the wide distribution of lifetimes (in the range of 100–700 ps) for 40 cresyl violet molecules that undergo interfacial electron transfer. This distribution provides



**Figure 4.** Atomic force microscope (AFM) image ( $250 \text{ nm} \times 250 \text{ nm}$ ) of a sputter-coated indium tin oxide (ITO) surface taken in contact mode. The features in nanometer-spatial scale are evident.

very detailed information. On the basis of Figure 3, kinetics measured on large ensembles of molecules would exhibit 20 exponentials, which are impossible to resolve using conventional measurements on large ensembles of molecules. In addition to these molecules, we also observed some molecules not undergoing electron transfer, but rather pure radiative decays with lifetimes longer than 2 ns. Interfacial electron transfer on the subpicosecond time<sup>16,22,26,34,41</sup> is also possible in this system. However, single molecules involved in such fast electron transfer processes are difficult to image because of the low emission quantum yields. In addition, we cannot measure lifetimes shorter than 100 ps because of the 160-ps (fwhm) instrument response time. Although the distribution of the electron transfer rates we observed may not be a complete distribution, our observations do reveal that the origin of multiexponential behavior of this system arises from the heterogeneity of site-specific molecular interactions.

In investigating the origin of site heterogeneity, we found no correlation between emission peak positions and fluorescence lifetimes. Electron transfer rates were determined by electronic coupling between the excited state of the dye molecule and the conduction band of the semiconductor, the driving force, and the solvent reorganization energy.<sup>42</sup> The emission peak positions of dye molecules are not necessarily directly related to these physical parameters. Finally, we used an AFM to map the ITO surfaces. Figure 4 displays a 250 × 250-nm<sup>2</sup> contact AFM image of the surface of an ITO film. The image shows distinct features on the nanometer scale, making a variety of sites available on the surface. We are currently working on correlating topological information with the electron transfer rates.

## Conclusions

Single-molecule chemical reaction kinetics was measured for interfacial electron transfer from photoexcited cresyl violet molecules to the conduction band or energetically accessible surface electronic states of ITO. In this system, each single molecule exhibited single-exponential electron transfer kinetics, and the decay rates were different for the single molecules at different sites. A wide distribution of site-specific electron transfer rates was determined. This work revealed that the physical origin of multiexponential kinetics of electron transfer on the semiconductor surface of ITO was the inhomogeneity of molecular interactions. We anticipate that inhomogeneity is the general origin of the multiexponential kinetics for the interfacial electron transfer in other dye sensitization systems. There was no distinct correlation between the electron transfer rates and the emission peak positions for the single molecules in this system. Although the rates of electron transfer of similar systems are strongly dependent on sample preparation<sup>14–21</sup> and a systematic study is required to reveal the detailed mechanism of electron transfer in this system, we demonstrated that single-molecule experiments provide detailed information not obtainable from experiments conducted on large ensembles of molecules. The ability to measure the rate of single-molecule chemical reactions in specific environments creates new opportunities for studying chemical dynamics in many heterogeneous systems.

**Acknowledgment.** We thank Professors Joseph Hupp, Prashant Kamat, and Nathan Lewis for helpful discussions. Pacific Northwest National Laboratory is operated for the U.S. Department of Energy (DOE) by Battelle. The research was supported by DOE's Office of Basic Energy Sciences, Chemical Sciences Division, Fundamental Interaction Branch.

## References and Notes

- (1) Betzig, E.; Chichester, R. J. *Science* **1993**, 262, 1422.
- (2) Trautman, J. K.; Macklin, J. J.; Brus, L. E.; Betzig, E. *Nature* **1994**, 369, 40.
- (3) (a) Xie, X. S. *Acc. Chem. Res.* **1996**, 29, 598. (b) Xie, X. S.; Bian, R. X.; Dunn, R. C. In *Focus on Multidimensional Microscopy* 1997; Chen, P. C., Hwang, P. P., Wu, J. L., Wang, G., Kim, H., Eds.; World Scientific: Singapore, 1997, Vol. 1. (c) Dunn, R. C.; Holtom, G. R.; Mats, L.; Xie, X. S. *J. Phys. Chem.* **1994**, 98, 3094.
- (4) Xie, X. S.; Dunn, R. C. *Science* **1994**, 265, 361.
- (5) Ambrose, W. P.; Goodwin, P. M.; Martin, J. C.; Keller, R. A. *Science* **1994**, 265, 364.
- (6) Bian, R. X.; Dunn, R. C.; Xie, X. S.; Leung, P. T. *Phys. Rev. Lett.* **1995**, 75, 4772.
- (7) (a) Nie, S.; Chiu, D. T.; Zare, R. N. *Science* **1994**, 266, 1018. (b) Funatsu, T.; Harada, Y.; Tokunaga, M.; Saito, K.; Yanagida, T. *Nature* **1995**, 374, 555. (c) Eigen, M.; Rigler, R. *Proc. Natl. Acad. Sci. U.S.A.* **1994**, 91, 5740.
- (8) Macklin, J. J.; Trautman, J. K.; Harris, T. D.; Brus, L. E. *Science* **1996**, 272, 255.
- (9) Lu, H. P.; Xie, X. S. *Nature*, **1997**, 385, 143.
- (10) For reviews, see: (a) Moerner, W. E. *Science* **1994**, 265, 46. (b) Moerner, W. E.; Basche, T. *Angew. Chem.* **1993**, 32, 457. (c) Orrit, M.; Bernard, J.; Personov, R. I. *J. Phys. Chem.* **1993**, 97, 10256. (d) Myer, A. B.; Tchenio, P.; Zgierski, M. Z.; Moerner, W. E. *J. Phys. Chem.* **1994**, 98, 10377. (e) Wild, U. P.; Croci, M.; Cutler, F.; Pirotta, M.; Renn, A. *J. Lumin.* **1994**, 60–61, 1003.
- (11) (a) Schmidt, Th.; Schutz, G. J.; Baumgartner, W.; Gruber, H. J.; Schindler, H. J. *J. Phys. Chem.* **1995**, 99, 17662. (b) Dickson, R. M.; Norris, D. J.; Tzeng, Y.-L.; Moerner, W. E. *Science* **1996**, 274, 966. (c) Ha, T.; Enderle, Th.; Chemla, D. S.; Selvin, P. R.; Weiss, S. *Phys. Rev. Lett.* **1996**, 77, 3979.
- (12) (a) Collinson, M. M.; Wightman, R. M. *Science* **1995**, 268, 1883. (b) Bard, A. J.; Fan, F.-R. F. *Acc. Chem. Res.* **1996**, 29, 572.
- (13) (a) Xue, Q. F.; Yeung, E. S. *Nature* **1995**, 373, 681. (b) Craig, D. B.; Arriaga, E. A.; Wong, C. Y.; Lu, H.; Dovichi, N. J. *J. Am. Chem. Soc.* **1996**, 118, 5245.
- (14) Lewis, N. S. *Am. Sci.* **1995**, 83, 534.
- (15) Hagfeldt, A.; Gratzel, M. *Chem. Rev.* **1995**, 95, 49.
- (16) Willig, F. In *Surface Electron Transfer Processes*; Miller, R. J. D., McLendon, G. L., Nozik, A. J., Schmickler, W., Willig, F., Eds.; VCH Publishers: New York, 1995.
- (17) Gratzel, M. *Heterogeneous Photochemical Electron Transfer*; CRC Press, Inc.: Boca Raton, FL, 1987.
- (18) Watanabe, T.; Fujishima, A.; Honda, K. *Energy Resources Through Photochemistry and Catalysis*; Gratzel, M., Ed.; Academic Press: New York, 1983.
- (19) Kamat, P. V. *Chem. Rev.* **1993**, 93, 267.
- (20) West, W.; Gilman Jr., P. B. In *The Theory of the Photography Process*; James, H. T., Eds.; MacMillan: New York, 1977.
- (21) Law, K. Y. *Chem. Rev.* **1993**, 93, 449.
- (22) Nozik, A. J.; Memming, R. J. *J. Phys. Chem.* **1996**, 100, 13061.
- (23) (a) Clark, W. D.; Sutin, D. J. *J. Am. Chem. Soc.* **1977**, 99, 4676. (b) Gleria, M.; Memming, R. Z. *Phys. Chem., Neue Folge* **1975**, 98, 303. (c) Matsumura, M.; Mitsuda, K.; Yoshizawa, N.; Tsubomura, H. *Bull. Chem. Soc. Jpn.* **1981**, 54, 692. (d) Spanhel, L.; Anderson, M. A. *J. Am. Chem. Soc.* **1991**, 113, 2826. (e) Hotchandani, S.; Bedja, I.; Kamat, P. V. *Langmuir* **1994**, 10, 17.
- (24) (a) Rossetti, R.; Brus, L. E. *J. Am. Chem. Soc.* **1984**, 106, 4336. (b) Fessenden, R. W.; Kamat, P. V. *J. Phys. Chem.* **1995**, 99, 12902.
- (25) Kietzmann, W. F.; Weller, H.; Vogel, R.; Nath, D.; Eichberger, R.; Liska, P.; Lehnert, J. *Mol. Cryst. Liq. Cryst.* **1991**, 194, 169.
- (26) (a) Willig, F.; Eichberger, R.; Sundaresan, N. S.; Parkinson, B. A. *J. Am. Chem. Soc.* **1990**, 112, 2702. (b) Burfeindt, B.; Hannappel, T.; Storck, W.; Willig, F. *J. Phys. Chem.* **1996**, 100, 16463.
- (27) Liang, Y.; Ponte Goncalves, A. M. *J. Phys. Chem.* **1985**, 89, 3290.
- (28) (a) Kamat, P. V.; Fox, M. A. *Chem. Phys. Lett.* **1983**, 102, 379. (b) Kamat, P. V.; Chauvet, J. P.; Fessenden, R. W. *J. Phys. Chem.* **1985**, 89, 3290. (c) Kamat, P. V.; Chauvet, J. P.; Fessenden, R. W. *J. Phys. Chem.* **1986**, 90, 1389. (d) Vinodgopal, K.; Hua, X.; Kamat, P. V.; Bedja, I.; Hotchandani, S. *J. Phys. Chem.* **1994**, 98, 9137. (e) Dahlgren, R. L.; Lappin, A. G.; Patterson, L. K.; Kamat, P. V. *J. Phys. Chem.* **1995**, 99, 10883. (f) Liu, D.; Kamat, P. V. *J. Chem. Phys.* **1996**, 105, 965.
- (29) (a) Hashimoto, K.; Hiramoto, M.; Sakata, T. *J. Phys. Chem.* **1988**, 92, 4272. (b) Hashimoto, K.; Hiramoto, M.; Lever, A. B.; Sakata, T. *J. Phys. Chem.* **1988**, 92, 1016. (c) Hashimoto, K.; Hiramoto, H.; Kajiwara, T.; Sakata, T. *J. Phys. Chem.* **1988**, 92, 4636. (d) Hashimoto, K.; Hiramoto, M.; Sakata, T. *Chem. Phys. Lett.* **1988**, 148, 215. (e) Sakata, T.; Hashimoto, K.; Hiramoto, M. *J. Phys. Chem.* **1990**, 94, 3040.
- (30) (a) Duonghong, D.; Borgarello, E.; Gratzel, M. *J. Am. Chem. Soc.* **1981**, 103, 4685. (b) Duonghong, D.; Ramsden, J.; Gratzel, M. *J. Am. Chem. Soc.* **1982**, 104, 2977. (c) Moser, J.; Gratzel, M. *J. Am. Chem. Soc.* **1983**, 105, 6547. (d) Moser, J.; Gratzel, M. *J. Am. Chem. Soc.* **1984**, 106, 6557. (e) Desilvestro, J.; Gratzel, M.; Kavan, L.; Moser, J.; Augustynski, J. *J. Am. Chem. Soc.* **1985**, 107, 2988. (f) Vrachnou, E.; Vlachopoulos, N.; Gratzel, M. *J. Chem. Soc., Chem. Commun.* **1987**, 868. (g) Liska, P.; Augustynski, J.; Gratzel, M. *J. Am. Chem. Soc.* **1988**, 110, 1216. (h) O'Regan, B.; Gratzel, M. *Nature* **1991**, 353, 737.

- (31) Lu, H.; Prieskorn, J. N.; Hupp, J. T. *J. Am. Chem. Soc.* **1993**, *115*, 4927.
- (32) Ford, W. E.; Rodgers, M. A. *J. Phys. Chem.* **1995**, *99*, 5139.
- (33) Tamai, N.; Matsuo, H.; Yamazaki, T.; Yamazaki, I. *J. Phys. Chem.* **1992**, *96*, 6550.
- (34) Rehm, J. M.; McLendon, G. L.; Nagasawa, Y.; Yoshihara, K.; Moser, J.; Gratzel, M. *J. Phys. Chem.* **1996**, *100*, 9577.
- (35) Parkinson, B. A.; Spitler, M. T. *Electrochim. Acta* **1992**, *37*, 943.
- (36) Sereno, L.; Silber, J. J.; Otero, L.; Bohorquez, M. V.; Moore, A. L.; Moore, T. A.; Gust, D. *J. Phys. Chem.* **1996**, *100*, 814.
- (37) When a nonradiative decay rate is much faster than a radiative decay rate, the fluorescence decay rate is dominated by the nonradiative decay and approximately equal to the nonradiative decay rate.
- (38) (a) Blackburn, R. L.; Johnson, C. S.; Hupp, J. T. *J. Am. Chem. Soc.* **1991**, *113*, 1060. (b) Doorn, S. K.; Blackburn, R. L.; Johnson, C. S.; Hupp, J. T. *Electrochim. Acta* **1991**, *36*, 1775.
- (39) (a) Lukosz, W.; Kunz, R. E. *Opt. Commun.* **1977**, *20*, 195. (b) Lukosz, W.; Kunz, R. E. *J. Opt. Soc. Am.* **1977**, *67*, 1607.
- (40) For a review, see Blandamer, M. J.; Fox, M. F. *Chem. Rev.* **1970**, *70*, 59.
- (41) (a) Lanzafame, J.; Min, L.; Miller, R. J. D.; Muentner, A.; Parkinson, B. *Mol. Cryst. Liq. Cryst.* **1991**, *194*, 287. (b) Lanzafame, J. M.; Miller, R. J. D.; Muentner, A. A.; Parkinson, B. A. *J. Phys. Chem.* **1992**, *96*, 2820.
- (42) Marcus, R. A.; Sutin, N. *Biochim. Biophys. Acta* **1985**, *811*, 265.